UNIVERSITY OF CALIFORNIA,
IRVINE

Control and Predictability of Near-Field Electrospinning

THESIS

submitted in partial satisfaction of the requirements
for the degree of

MASTER OF SCIENCE

in Engineering

by

Lanchun He

Thesis Committee:
Professor Marc Madou, Chair
Dr. Lawrence Kulinsky
Professor Chin Lee

2017

DEDICATION

To

my parents and friends

for their love, support and encouragement

TABLE OF CONTENTS

LIST OF FIGURES

ACKNOWLEDGMENTS

I would like to express the deepest appreciation to my advisor, Professor Marc Madou for providing me the incredible patience and supporting me go further in my research. I will never forget him for the recommendations he sent for me. Also, his humor build a pleasant and comfortable atmosphere in BioMEMS group where I spent a colorful life in last two years.

I would like to thank my committee members, Professor Chin Lee, who gives me an opportunity to get into UCI and Materials and Manufacturing Technology. I learnt a lot and experienced a brand-new life here. As a director of MMT, he gave me many helpful advice in career decision.

In addition, a thank you to Dr. Lawrence Kulinsky, who taught me a lot about biomedical devices, and who were so kind to be a member of my committee. I love the way he presented in class.

I also would like to express my sincere gratitude to BioMEMS group, they were really kind and nice to me. I met lots of friends there. We discussed about researches together, played beach ball together and celebrated birthday together. Thanks for the time they companied with me.

Finally, I hope to thank my parents, a laborious couple who took effort to bring up their daughter. They supported me to go abroad, see the world and experience a different life. Their encouragements helped me get over difficulties and loneliness. Thanks for their support, understand and love.

ABSTRACT OF THE THESIS

Control and Predictability of Near-Field Electrospinning

By

Lanchun He

Master of Science in Engineering

University of California, Irvine, 2017

Professor Marc Madou, Chair

Nanofiber produced by electrospinning has been used in a wide range. However, in traditional electrospinning, a bending instability occurs as the fiber travels from the needle to a collecting substrate due to charge interactions which causes the fibers to deposit on the collector randomly. A new form electrospinning called near-field electrospinning(NFES) has been discovered in last decades. This technology allows a good control of nanofibers, makes it feasible to draw nanofibers in a certain pattern without bending instability happened in traditional electrospinning. Also, NFES decreases voltage applied to setup from thousands of volts to hundreds of volts, making the electrospinning process cheaper and safer. But this new form technology still has limitations. Since NFES decreases working distance between needle and substrate to millimeter scale and since polymer droplet size is small. Getting a good control of electrospinning initiation process is difficult to achieve. This thesis demonstrates the feasibility of using electrostatic forces to get a good control of initiation process and make the whole process predictable. In addition, relationship between thickness of nanofibers and key experimental parameters such as initiation tip

size, working distance, voltage and droplet size are studied in this thesis using finite element analysis.

INTRODUCTION

Background and Objectives

Electrospinning is a technique for the fabrication of polymeric micro- and nanofibers that uses a large electric field to stretch a polymer droplet into fibrous structures with applications in filtration systems, scaffolds, and micro- and nanodevices [1,2]. In traditional electrospinning, a bending instability occurs as the fiber travels from the needle to a collecting substrate due to charge interactions within the polymer jet. This bending instability causes the fibers to deposit on the collector with random orientations, resulting in a 3D interwoven nanofibers [3].

Within the last decade, a new form of electrospinning has emerged called the near-field electrospinning (NFES) [1]. Although NFES utilizes the same mechanism as traditional electrospinning, it is inherently a different fabrication process. While traditional electrospinning has been used as a means of creating textile like nanostructure mats, NFES is a nano-writing fabrication process, which is capable of creating controlled continuous fibrous patterns. In NFES the bending instabilities are eliminated, allowing the development of such patterns by positioning the collector significantly closer to the needle (<3 mm) than in conventional electrospinning (10-30 cm), and scaling down the voltage applied to the needle (600 – 1000 V vs 10 -30 kV) [1, 4, 5]. Due to the difference in characteristic length between NFES and traditional electrospinning the latter sometimes it's referred as far field electrospinning (FFES) [6].

The main advantages of NFES as a nano-writing system, compared to other contemporary systems, are the remarkable flexibility and relatively low cost, it allows a certain pattern of

nanowires [6] (Figure 1). NFES is compatible with most polymer solutions with a few exceptions due to their electrical permittivity, charge conductivity and/or viscoelasticity. However, these restrictions could be often easily overcome through changes in the solvent, addition of salts and/or addition of more elastic polymers. NFES also is one of the few nano-writing techniques that can fabricate suspended structures, while avoiding common problems such as stiction that often adversely affects wet fabrication processes. A variation of NFES was developed by our group at the University of California in Irvine, we notice that it is possible to fabricate thinner fibers by inducing jet initiation process electrostatically compared to traditional NFES by mechanically stretching the electrospun fibers. This reduction in diameter it's achieved by reducing the needle-to-substrate distance to less than 1 mm and the voltage to the range of 200 V to 800 V, and by optimizing the viscoelasticity of the polymer solution as described in reference [7].

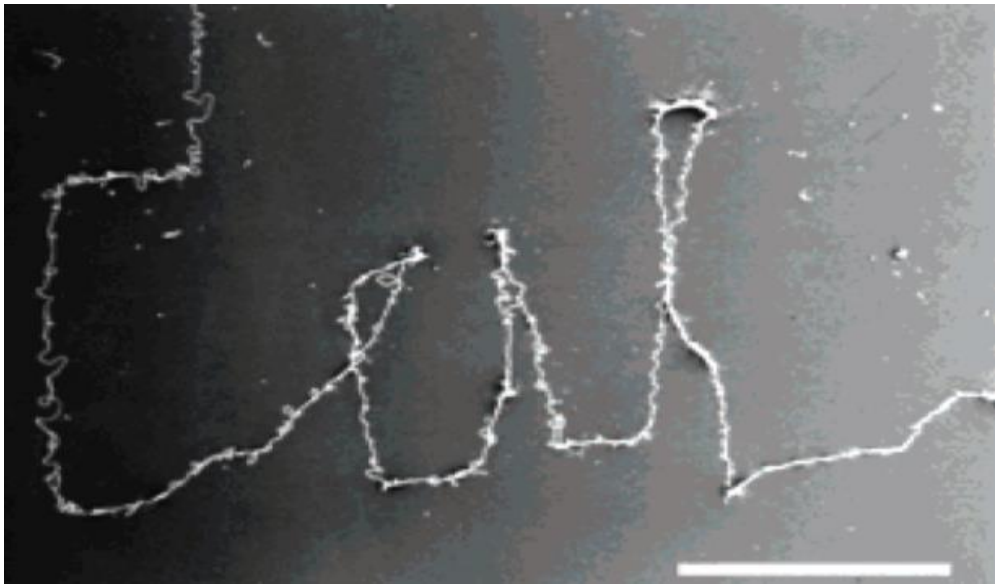

Figure 1. Poly (ethylene oxide) fibers fabricated with NEFS patterning the three-character "Cal" logo. Scale bar, 1 mm [1].

Although NFES is very promising nano-writing methods, certain difficulties in understanding and controlling the deposition of the electrospun fibers have slowed down its automation and commercialization. Main challenges include the controllability and reproducibility of polymer-substrate interactions and the lack of a reliable method for initiating the fiber jet, both factors that affect the uniformity and variation of the fiber's diameter. Unlike FFES, the electric field in near-field range is not strong enough to break the surface tension of the polymer droplet and thus automatically initiate the polymer jet deposition [6]. Therefore, NFES requires alternative methods to induce an instability to the polymer droplet meniscus to initiate the jet. Currently, the most common method for jet initiation in NFES it's by physically touching the meniscus to break the surface tension of the droplet. However, this method is difficult to control, and unreliable for producing fibers with well-defined dimensions, in addition to producing thicker fibers, with diameters above 1 μm [7]. Furthermore, by integrating NFES with the Carbon-MEMS microfabrication process, that consists of UV photolithography of carbon precursor followed by a pyrolysis treatment at 900 °C under an inert N2 environment, this group has reported on the development of carbon devices based on suspended carbon nanofibers [6,7,8].

This work demonstrates the feasibility of using electrostatic forces as a reproducible method for the initiation of the polymer fiber jet in NFES. The experimental setup, shown in figure 2, allows us to employ the electric field to substantially facilitate the electrostatic initiation of polymer fibers. The fibers developed via this new method are on average, an order of magnitude thinner and have significantly narrower variations in diameter as compared to those fabricated using physical contact initiation. Key fabrication parameters, including the working distance, size of initiation tip, droplet size, and applied voltage were

varied to experimentally determine their efficacy in electrostatic jet initiation. Numerical Finite Element models were implemented to visualize the effects of the afore-mentioned parameters on altering the shape and intensity of the electric field. The experimental results, verified by the numerical models, indicate that based on the applied voltage, we will be able to reliably predict the electrostatic field and the critical distance at which the fiber initiation process takes place. Such predictability shows the promise for a fully controllable near-filed electrospinning process and consequently paves the way for an automated nano-writing technique.

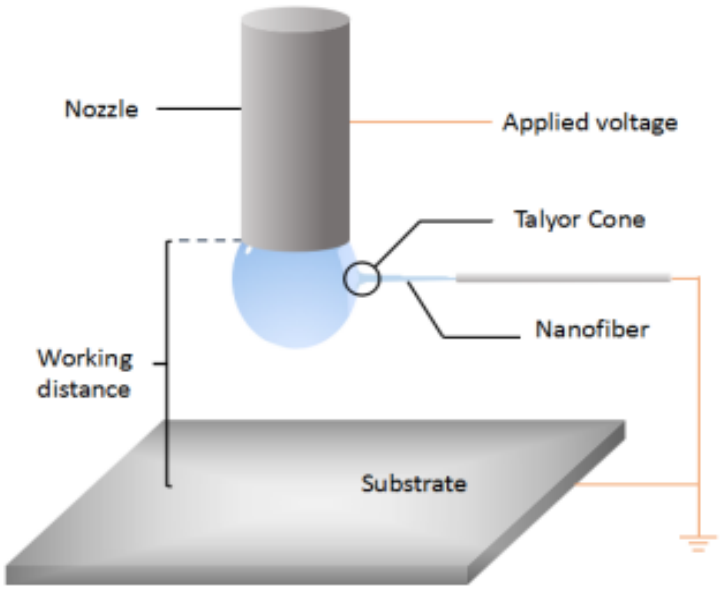

Figure 2. Schematic of electrostastic initiation of NFES.

Thesis Outline

The thesis is organized in six chapters to describe the characterization of nanofibers generated by NFES. Chapter 1 introduces the background of far-field electrospinning and near-field electrospinning. Chapter 2 describes generation process of nanofibers by using NFES and compares different initiation modes of fiber generation. Chapter 3 verifies the rightness of numerical simulation. Chapter 4 uses finite element analysis to study how distribution of electrical field will change with different experimantal parameters. Chapter 5 shows this side initiation NFES process is totally predictable. Chapter 6 illustrates conclution and future works.

CHAPTER 1: LITERATURE STUDY OF NEAR-FIELD ELECTROSPINNING

1.1 Far-field Electrospinning

Electrospinning is an advanced technology which produces nano-scale fibers with diameter form several nanometers to over 1mm. Because of its simple facilities, low cost and high tolerance with polymer solution, electrospinning has been one of the most popular methods to produce nanofibers. As early as 1934, Formlals et al. [9] applied a patent for an apparatus taking advantage of repulsion between surface charges of droplet to produce cellulose esters fibers. However, only a few publications about electropsinning published in late 90's. Only until these years, people revived interest in electrospinning because of the heat of nanotechnology studies. (Figure 1.1)

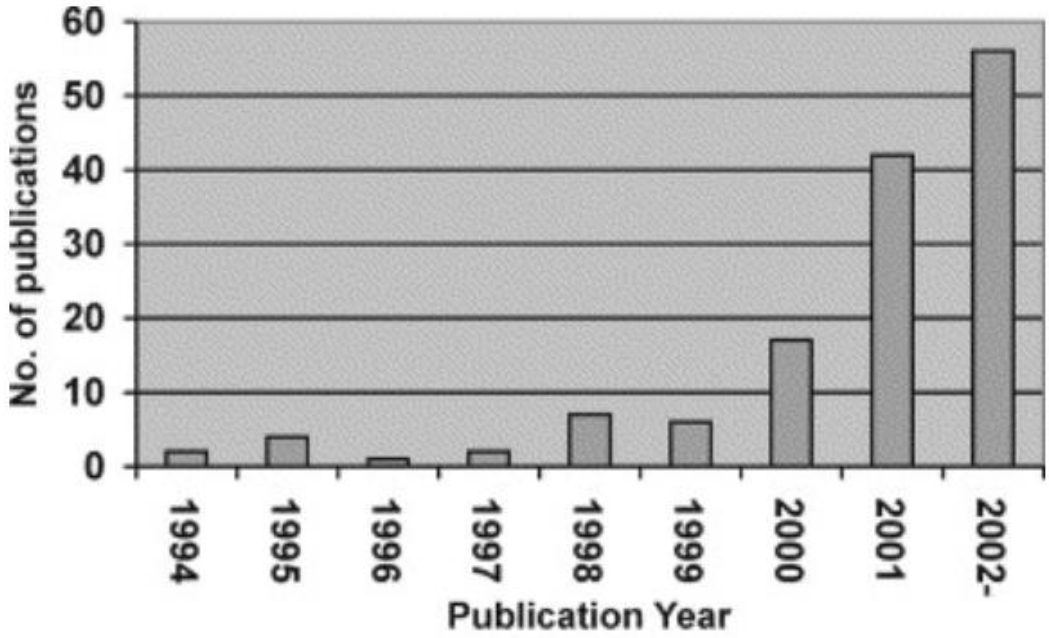

Figure 1.1 The annual number of publications about electrospinning [10]

.

Figure 1.2 shows a schematic of traditional electrospinning. A traditional electrospinning setup consists 3 main part: a metal needle contacts to reservoir of polymer solution, a collector (substrate) of polymer fibers and a high voltage power source.

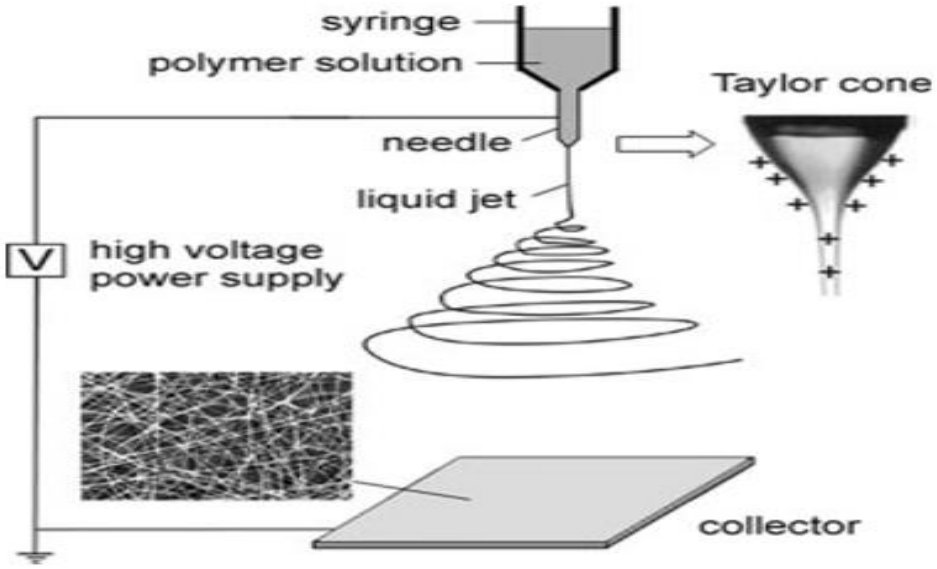

Figure 1.2 Schematic of traditional electrospinning [11].

Generally, a high voltage is applied between metal needle and substrate. This voltage charges the surface of droplet and leads to an electrostatic repulsion between particles on surface of droplet. Those particles also suffer from the electrical force generated by the strong electrical field between needle and substrate. When this sum of force overcomes the surface tension of solution, the hanging droplet is distorted into a cone shape which is commonly recognized as Taylor cone. [12, 2] Then this fiber is stretching and whipping and become a long and thin thread with the evaporation of

solvent. Finally, nanofibers are collected by the collector (substrate). Nanofibers produced by electrospinning shows in figure 1.3.

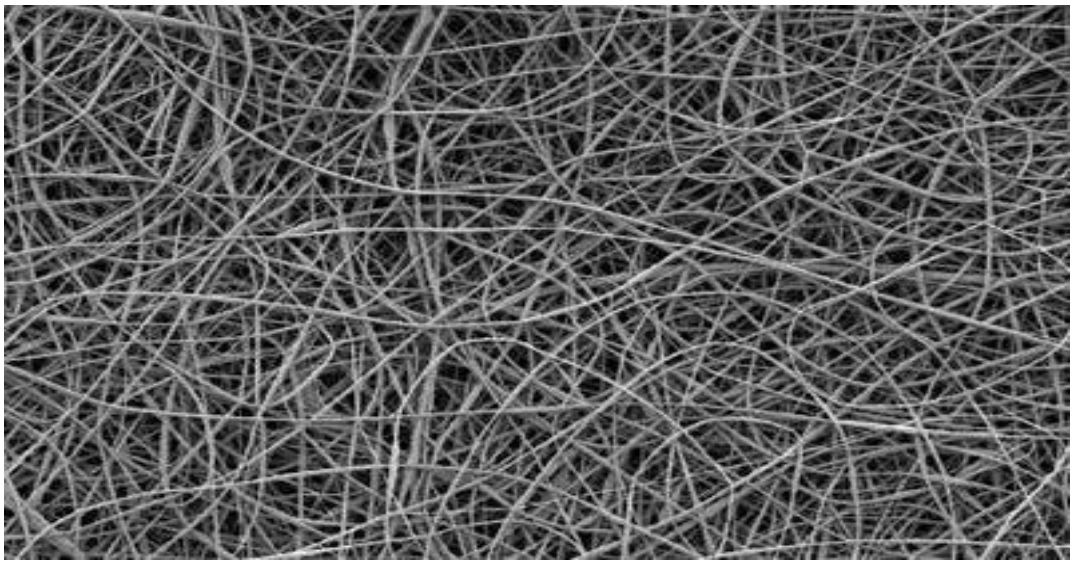

Figure 1.3. SEM of nanofibers produced by electrospinning. *Courtesy: Wikipedia.*

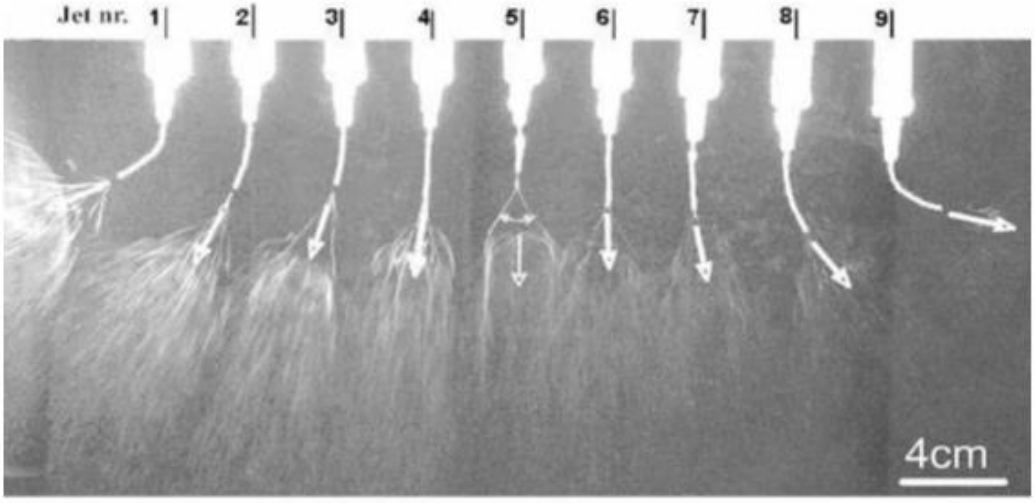

Figure 1.4. Multiple-jet electrospinning [13].

In addition to traditional electrospinning setup, modified setups are designed to improve performance of far field electrospinning. Theron et al [13] first develop a new

kind of far-field electrospinning with multiple jets since traditional far-field electrospinning has a low productivity (figure 1.4). However, electrical field interference among nozzle array may also be increased while multiple jets improve the rate of produce. In that case, design of multiple nozzles array should be careful to minimize the electrical interference.

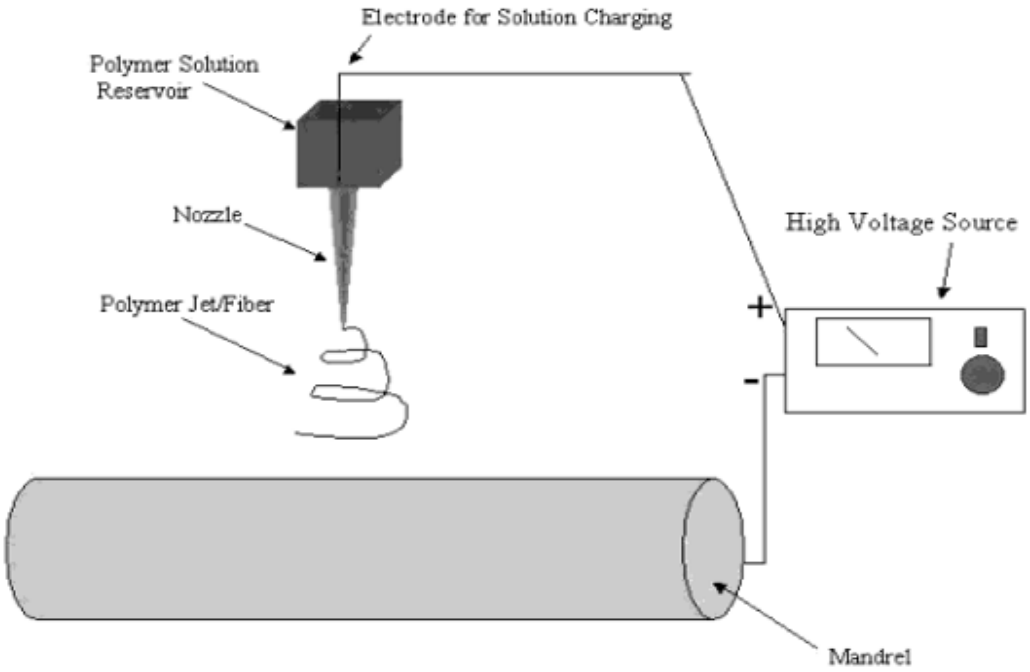

Figure 1.5. Far Field Electrospinning system with a rotating drum as a collector [14].

Alignment of nanofibers is another challenge for traditional electrospinning. In order to fix this problem, Kim et al. induced a rotating drum into traditional system [15]. And their work showed nanofibers are aligned as a uniform layer on rotation drum. This method is commercialized to collect oriented nanofibers. The schematic is show in figure 1.5.

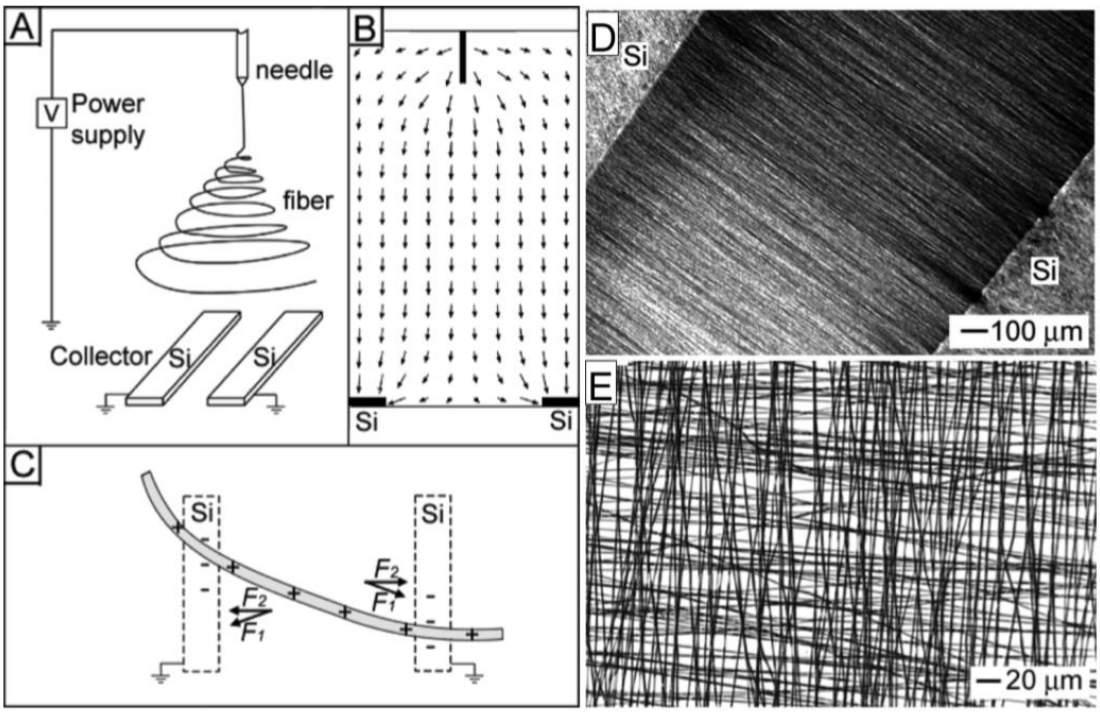

Figure 1.6. Schematic illustration of the setup for electrospinning with two parallel electrodes [16]

Li et al. designed another setup to collect aligned nanofibers [16]. He induced two parallel electrodes as the substrate. Those two electrodes changed distribution of electrical field and finally leaded to a vertical electrical field which improved the alignment of nanofibers. Setup, distribution of electrical field and SEM of nanofibers of this study are shown in figure 1.6.

There are many parameters influence performance of far field electrospinning. The inner factors refer to the characterization of polymer solution such as viscosity, electrical conductivity and elasticity. The outer factors include voltage applied on system, distance from substrate to metal needle, feeding rate of polymer solution, size of needle, temperature and humidity of environment [17].

1.2 Near-Field Electrospinning

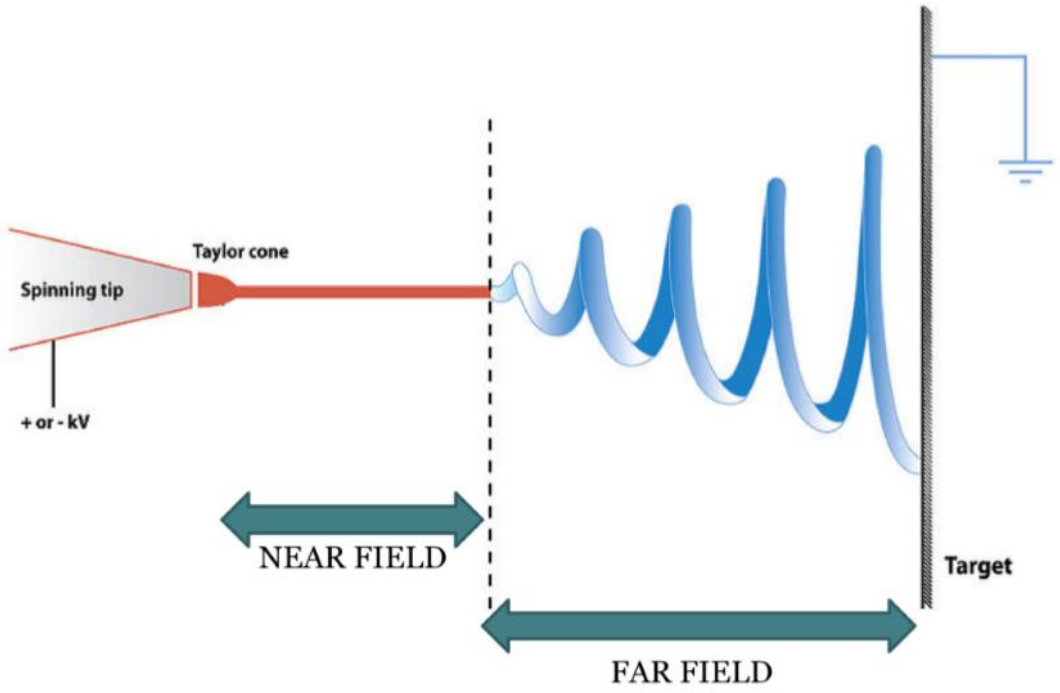

Figure 1.7. Schematic of near-field electrospinning and far-field electrospinning *Courtesy: Wikipedia.*

Compared to far field electrospinning, near-field electrospinning has a short distance between substrate and metal needle. Therefore, there is no need to apply extreme high voltage to trig the initiation of nanofibers. Near-field electrospinning downs the requirement of voltage from tens thousands of volts to hundreds of volts, and therefore produces nanofiber straightly without bending instability. This new form of electrospinning can be used in nano-writing, with this technology nanofibers are able to be drawn in specific pattern.

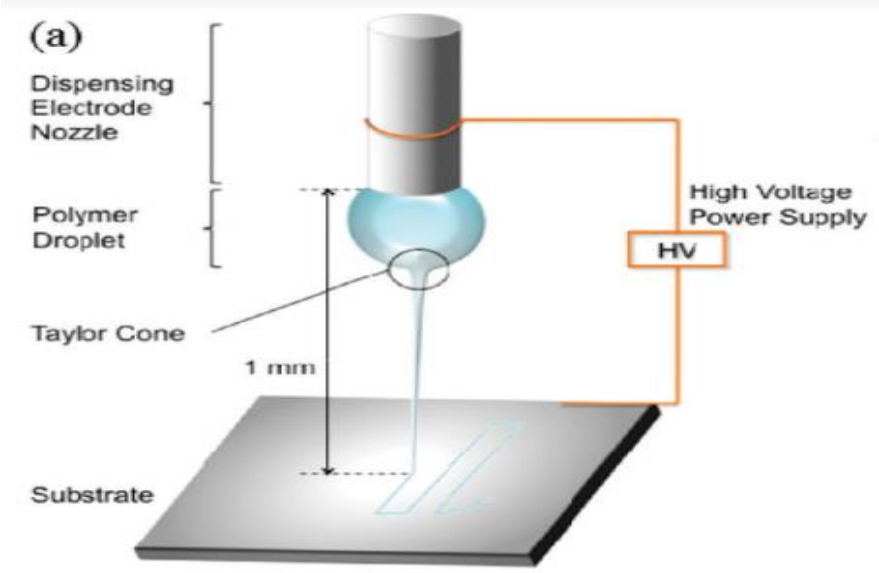

Figure 1.8. Traditional setup of near-field electrospinning [18].

Figure 1.8 shows the traditional setup of near-field electrospinning. Generally, repulsion between charges on surface of droplet is not strong enough to break the surface tension of in near-field electrospinning and thus automatically initiate the polymer jet deposition [6]. Therefore, NFES requires alternative methods to induce an instability to the polymer droplet meniscus to initiate the jet. Currently, physically touching the meniscus to break the surface tension of the droplet is the most common method for jet initiation [18]. However, this method is difficult to control, and unreliable for producing fibers with well-defined dimensions, in addition to producing thicker fibers, with diameters above 1 μm [7]. Key parameters of near-field electrospinning are the same as those for far-field electrospinning.

In this thesis, we improve traditional setup by inducing a glass-tip beside the droplet to focus the electrical field and take advantage of electrostatic force to produce nanofibers, schematic of our setup shows in introduction.

1.3 Conclusion

In this chapter, we introduce two way of electrospinning: Far-field electrospinning and Near-field electrospinning. Far-field has a bending instability because of the strong electrical field. There are several modified setups for FES to improve the performance. Near-field electrospinning can be used in nano-writing because there is no bending instability. It shorts the working distance and decreases the requirement of voltage, making the whole process cheaper and safer. Influence factors for both two electrospinning are pretty similar.

CHAPTER 2: NANOFIBER GENERATION PROCESS AND INITIATION MODE

2.1 Nanofiber Generation Process

From studies in electrohydrodynamic (EHD) jetting phenomena, it is known that when a voltage is applied between the dispensing nozzle and the grounded substrate, charges accumulate on the polymer meniscus reducing its radius of curvature. Jet initiation occurs when the sum of the hydrostatic and electrostatic pressure in the nozzle it's larger than the pressure induced by surface tension [19]:

$$\frac{1}{2}\varepsilon E^2 + \rho g h > \frac{2\sigma}{r_0}$$

Where ε it's the permittivity of the droplet, E the electric field, ρ the density of the fluid, g the acceleration of gravity, h the height difference between the nozzle tip and the liquid level on the reservoir, σ the surface tension of the liquid and r the radius of curvature of the droplet meniscus. After jetting from nozzle, nanofiber flows are stretched and elongated by outer strong electrical field and become into solid thread with the evaporation of solvent. Finally fall on the substrate.

2.2 Comparison of Initiation Modes

Towards a more controllable method for jet initiation that doesn't involve physical manipulation, we studied the conditions at which the electric field becomes strong enough to overcome the surface tension of the droplet. At first, we consider the main parameters influencing the moment at which a Taylor cone is formed in a NFES setup are the applied voltage and the distance from dispensing nozzle to grounded substrate. Initial experiments

to determine the conditions at which jet initiates on a bottom plate substrate were performed (figure 2.1). Taking the nozzle to substrate distance as 550 μm, the voltage was increase from 300 V to 700 V observing if jet initiation occurred. For bottom plate initiation, the success rate for 15 tests increased with increased voltage, with a maximum 60% success of jetting at 700 V (figure 2.3). While bottom electrical initiation has been used widely in NFES the need to apply higher voltages can introduce a whipping motion of the electrospun fibers similar to FFES (figure 2.2). Another initiation approach was to introduce a glass tip from the side of the polymer droplet (figure 2.4a). Additional parameter to consider for side initiation is diameter of the glass tip. Again, maintaining a 550 μm needle to substrate distance, the thickness of glass tip was 50 μm from the droplet. This glass tip focuses electrical field to its tip, therefore, the localize electric field it's strong enough to break the surface tension. Side initiation proved to be a more reliable method to initiate the deposition achieving a 100% success ratio at even the lower voltages. Thus, only the side electrical initiation can offer a high ratio of success and ordered fibers no matter what voltage was applied.

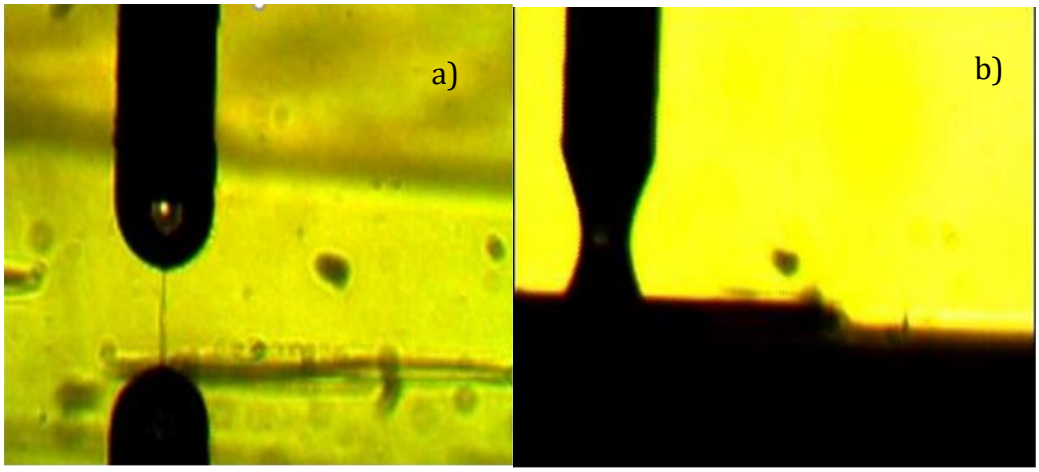

Figure 2.1. Bottom jet initiation: a) successful. b) unsuccessful.

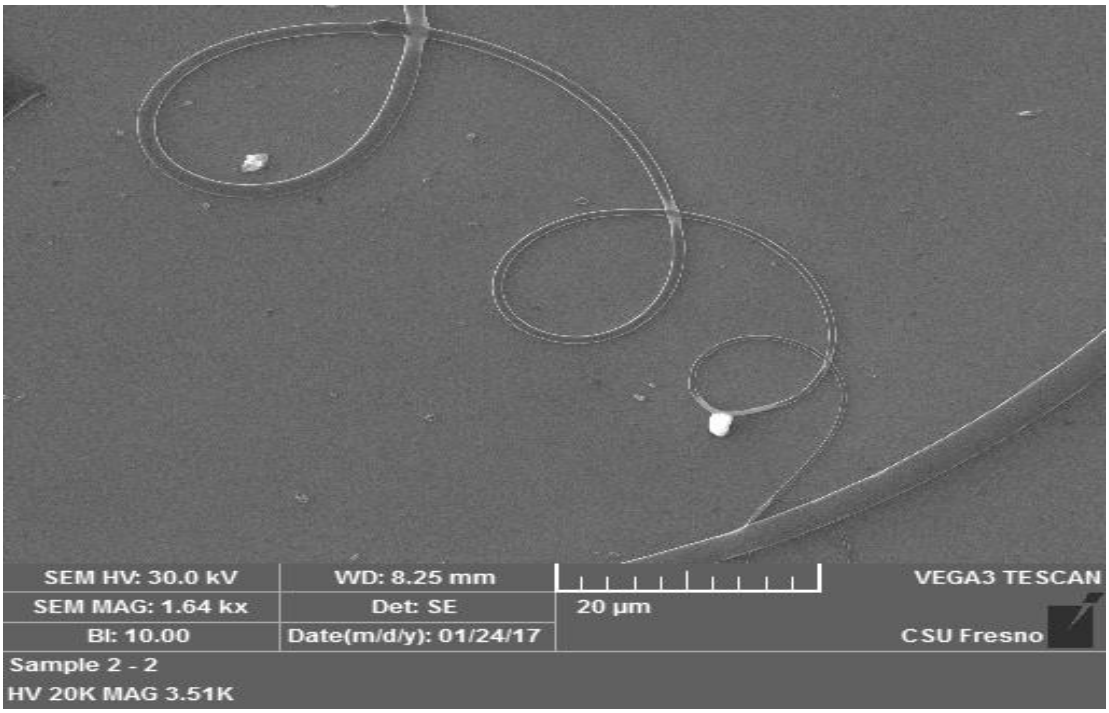

Figure 2.2. Whipping Motion of the Electrospun Nanofiber.

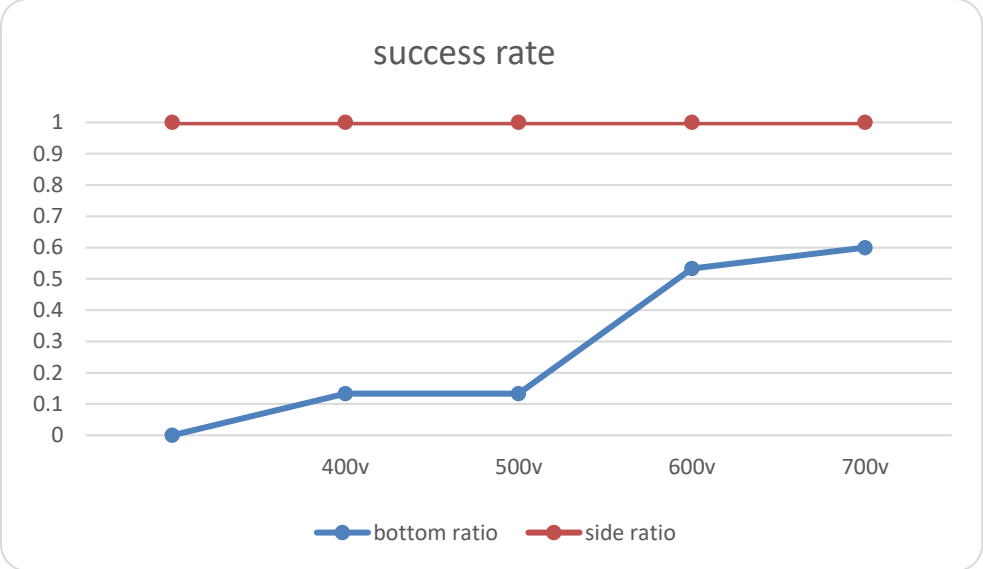

Figure 2.3. initiation success rate for bottom substrate initiation and side initiation.

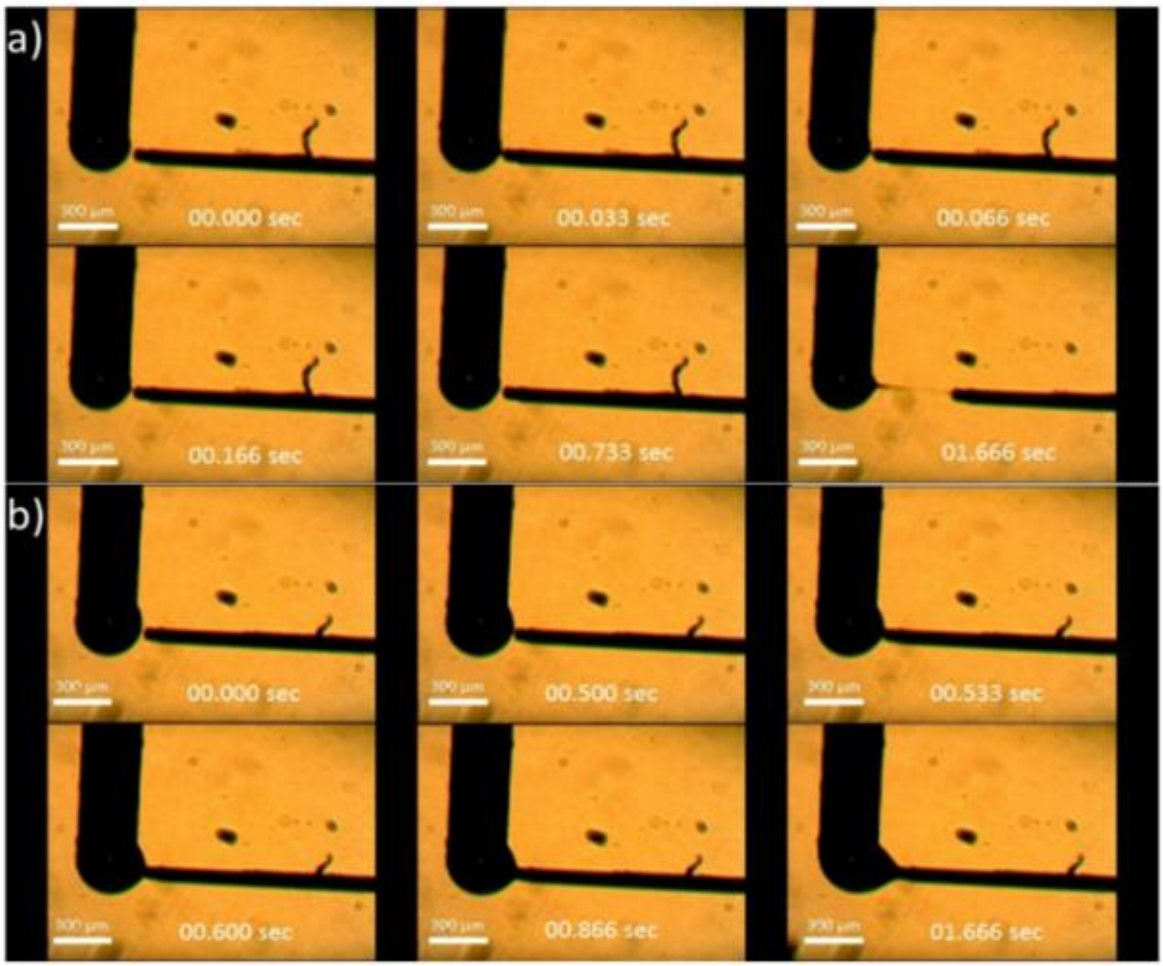

Figure 2.4. a) Side electrostatic initiation. b) manual initiation.

To test the performance of side electrostatic initiation, in comparison to manual poking initiation (figure 2.4b), fifteen fibers with each initiation method were deposited and subsequently pyrolyzed to obtain carbon fibers and their diameters measured with scanning electron microscope (SEM). Figure 2.5, presents the diameter distribution for the fibers fabricated with both electrostatic initiation and manual initiation methods. Figure 2.6 shows the nanowires in SEM. The average diameters of fibers produced by manual and electrostatic initiation were 1756 ± 253.8 nm and 693.4 ± 192.6 nm, respectively. Thus

clearly, by using electrical initiation, we can achieve a better control to produce more uniform fibers and thinner fibers.

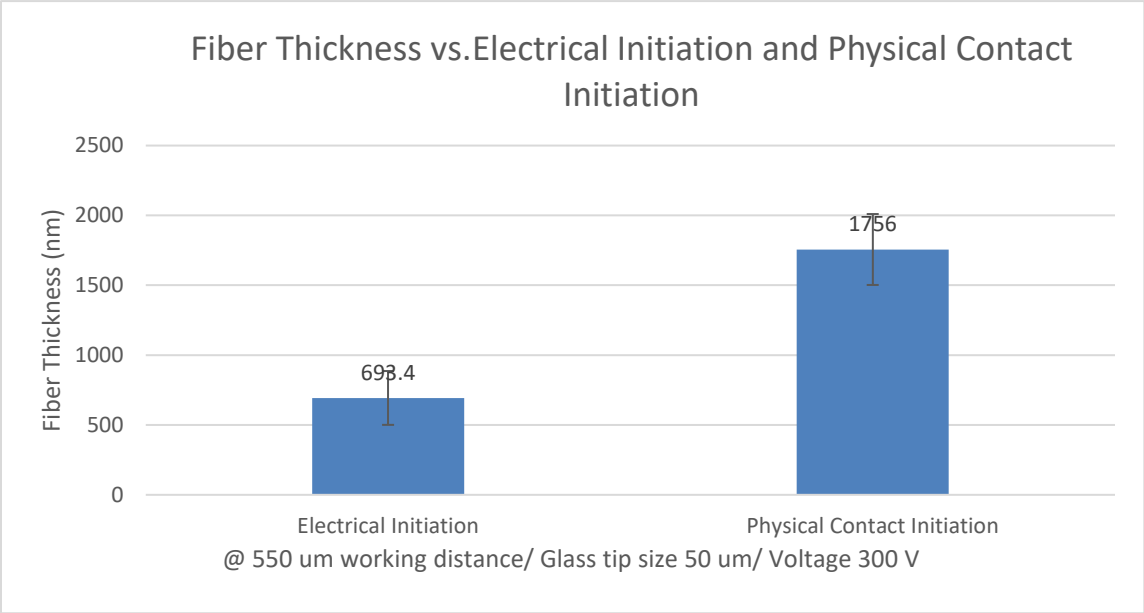

Figure 2.5. Diameter distribution of manual and electrostatic jet initiation

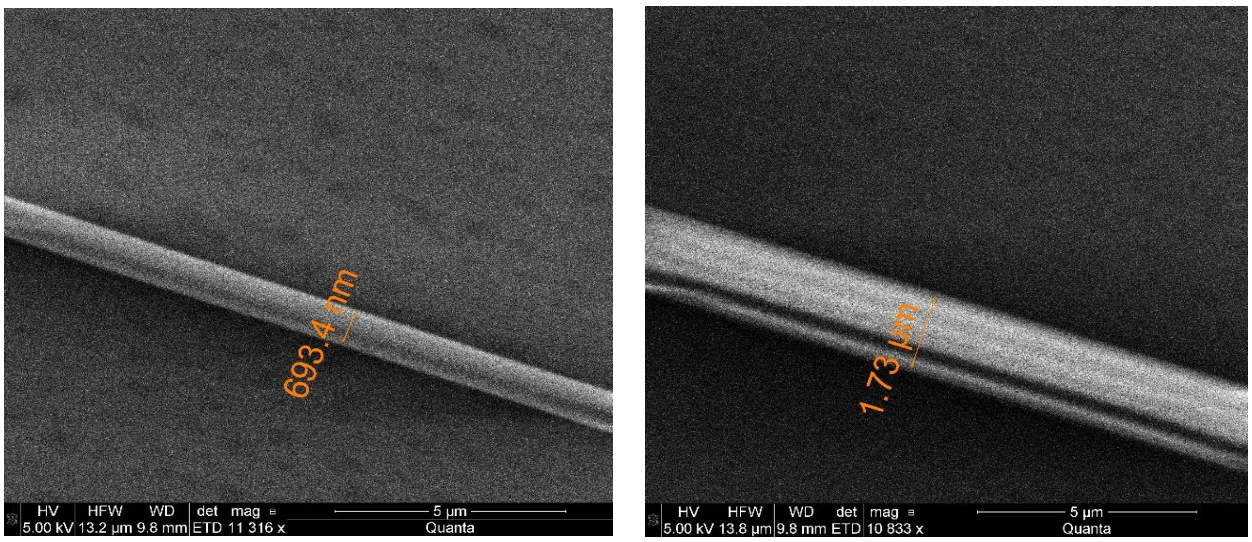

Figure 2.6. Thickness of nanofibers. a) thickness of nanofiber generated by electrical initiation. b) thickness of nanofiber generated by physical contact initiation

2.3 Conclusion:

In this Chapter, nanofiber generation process is described: when the sum of the hydrostatic and electrostatic pressure in the nozzle it's larger than the pressure induced by surface tension, the initiation of droplet will happen. Also, success rate of two initiation modes are compared. Side initiation NFES has a higher success rate than bottom initiation NFES. Nanofibers generated by physical contact initiation is thicker than those generated by electrical initiation.

CHAPTER 3: FEASIBILITY OF NUMERICAL ANALYSIS OF NFES SYSTEM

3.1 Feasibility Analysis of FEA Model of NFES System

To gain a better understanding on the electrostatic jet initiation phenomenon on NFES we performed a finite element analysis using the software COMSOL. First, we consider that when a droplet is put in an electrical field, it will be deformed by the electrical force. This deformation will change the radius of curvature of the droplet (figure 3.1). The relationship between the electric field, surface tension and deformation, D, is shown in equation below [20]:

$$D = \frac{9}{16}\frac{r_0 \varepsilon \varepsilon_0 E^2}{\sigma}$$

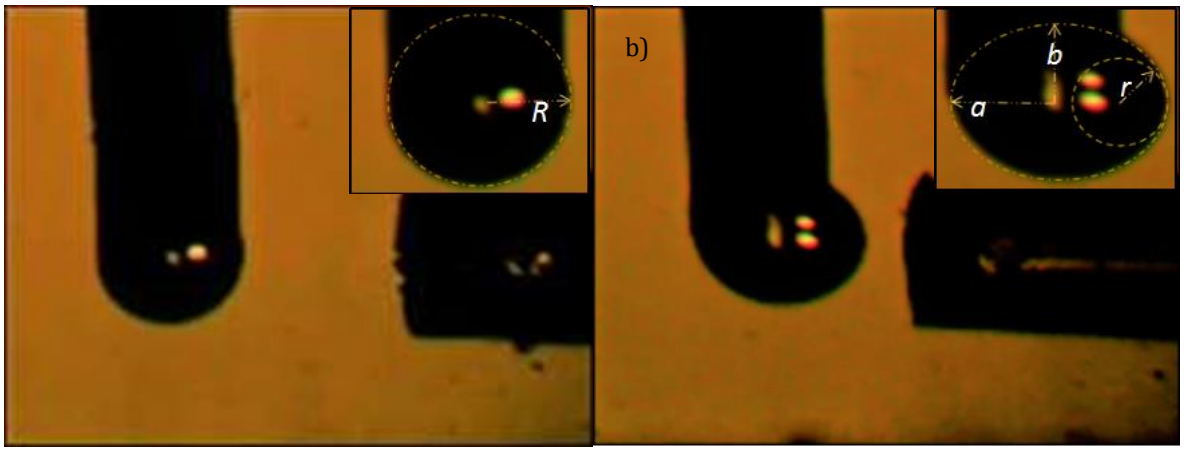

Figure 3.1. Radius of curvature change (a) No voltage. (b) Deformation after voltage application.

Additionally, the droplet deformation can be expressed as [21]:

$$D = \frac{a - b}{a + b}$$

Where a and b are ellipsoidal long and short axes respectively. For convenience of the simulation, we assume only 2D deformation, thus the area of the droplet before and after deformation should be keep the same. Moreover, the radius of curvature of long axis vertex of ellipse is b^2/a, which is also the radius of inscribed circle. These two relationships are shown in below equations:

$$\pi R^2 = \pi ab$$

$$\frac{b^2}{a} = r$$

a and b are the ellipsoidal long and short axes respectively, R is the radius of droplet before deformation. R refers to the radius of inscribed circle after deformation.

The deformation of the droplet under different applied electric fields it's observed in figure 3.2, where it is observed how the radius of curvature of the droplet is reduced with increased voltage. We record the whole initiation process and analyze video frame by frame, figure 3.2 shows the last frame picture of deformation of droplet before jet initiation. We assume that this frame shows the status when jet initiation starts.

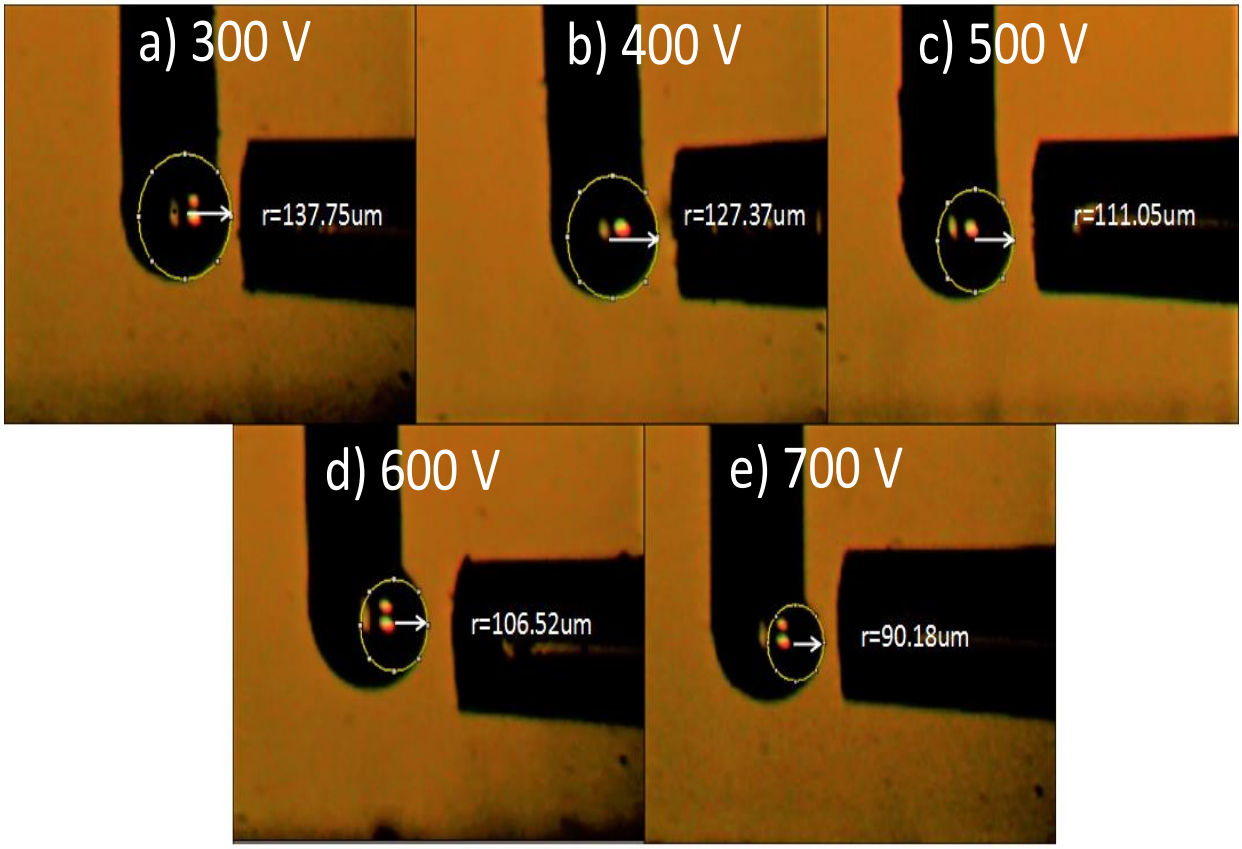

Figure 3.2. Deformation of droplet under an applied electric field before jet initiation. (a)-(e) 300-700 V

In order to obtain the localized electric field that induces jet initiation a COMSOL model (figure 3.3) was implemented. This model simulates the electrical field around the droplet when electrostatics initiation start. We acquire key parameters such as critical distance and droplet size from figure 3.2. Critical distance refers to the distance from critical point to glass tip. Critical point here refers to the point which has a smallest distance to the glass tip on the surface of droplet, this point suffers the biggest electrical force and jet initiation always starts at this point. For a droplet to substrate distance of 500 μm and thickness of glass tip is 300 μm, the value of the electric field in the x direction (between the droplet and glass-tip) with respect to the voltage it's obtained. Figure 3.4 shows the value of critical

electric field with applying voltage from 300V to 700V. Critical electrical field refers to the electrical field of critical point when electrostatic initiation happens.

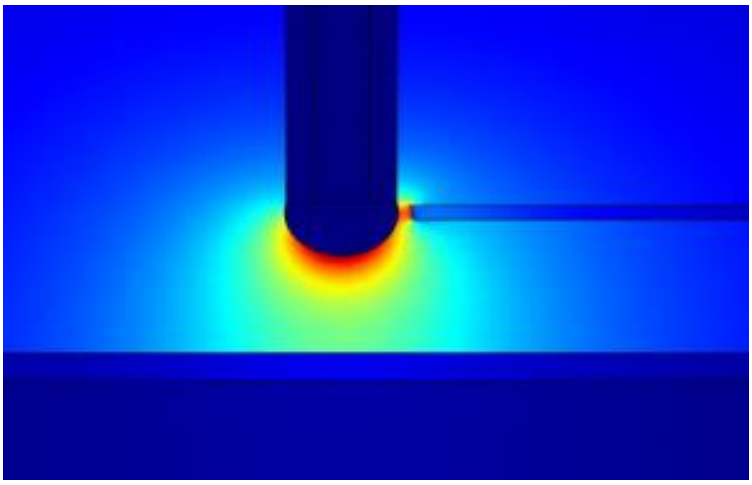

Figure 3.3. COMSOL model.

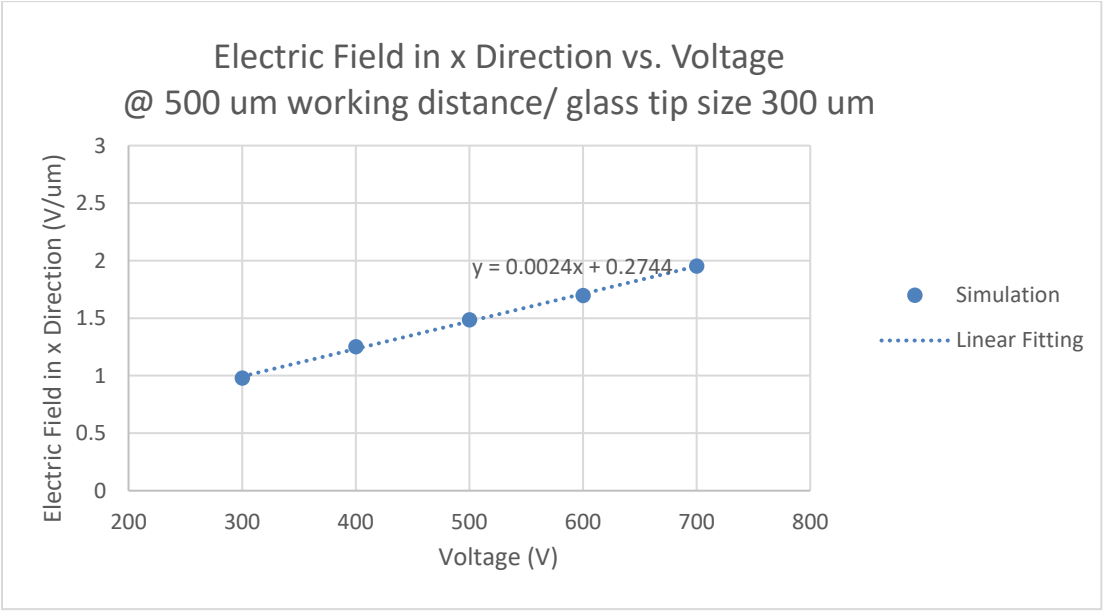

Figure 3.4. Localized electric field in x-direction vs voltage.

To prove the validity of our model, we assume that the surface tension of the droplet remains constant, and from equation 2 that $\sigma \propto E^2/D$. From the values obtained for the electric field and by measuring the radius of curvature as in figure 18, the ratio of E^2/D

it's plotted in figure 3.5, were it is observed how the value of the surface tension remains relatively unchanged.

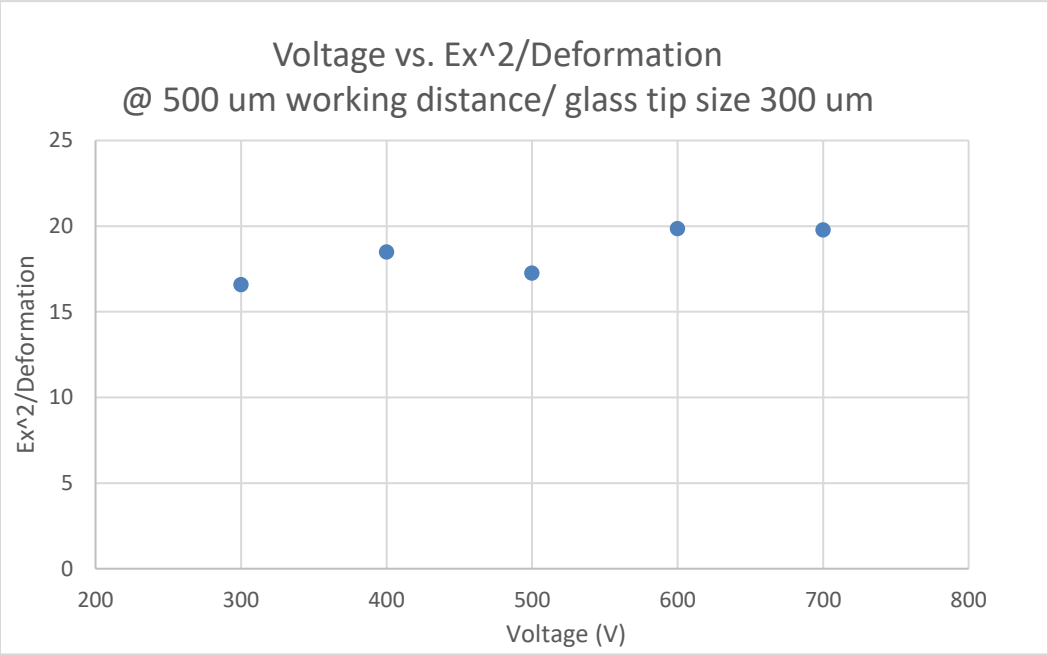

Figure 3.5. E^2/D vs. voltage.

Another way to prove the validity of the simulation it's by using equation [22] below to calculate E at the critical point of initiation and then compare it to the result of simulation. The results are shown in figure 3.6.

$$E(\xi) = \frac{2V}{(r + 2\xi - \xi^2/d)\ln(1 + 4d/r)}$$

E is the electrical field at critical point. ξ is the distance from needle to the point where generate the fiber, which in this case we assume it is 40um by approximation. r is the radius of bubble before deformation. d is the critical distance between glass tip and bubble when generate a fiber and V is the applied voltage on system

.

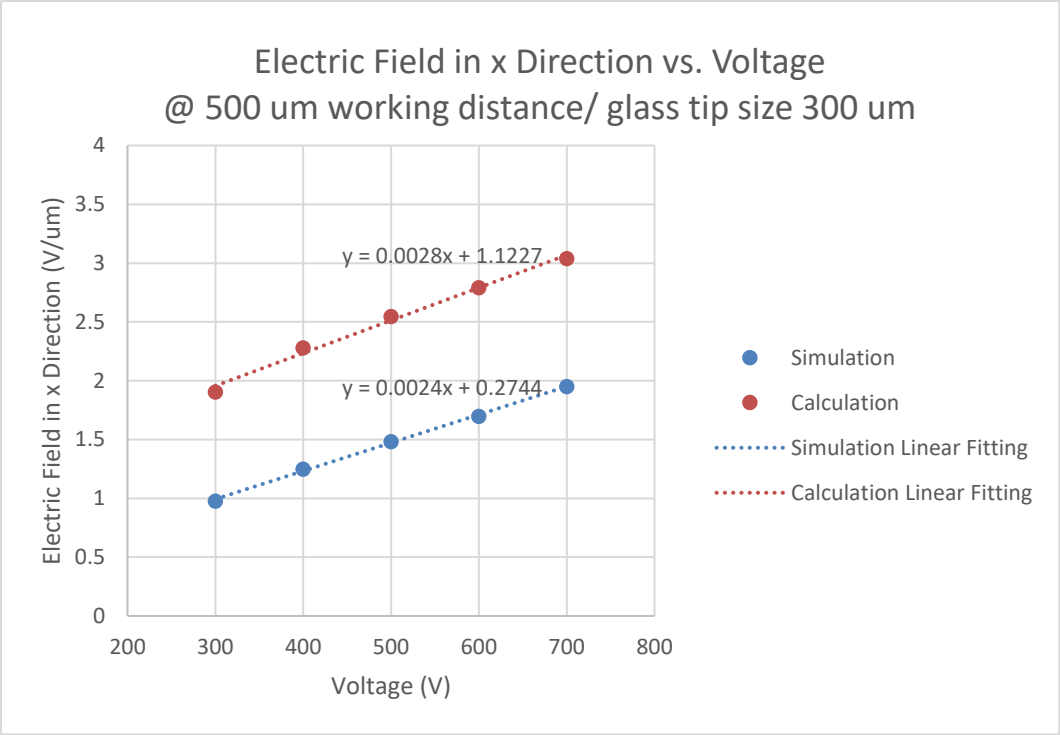

Figure 3.6. Simulated and calculated electric field.

The calculation result and simulation result of critical electrical field shown in figure 3.6 matches each other well with the slope linear fit of the simulated electric field being 0.0024 and for the calculated electric field being 0.0028. This conformity shows FEA mode was capable to be used in simulating electrical field of NFES system.

3.2 Conclusion:

In this chapter, two ways are introduced to show FEA model we built has a good ability to simulate electrical field of NFES system. One of them proves surface tension of droplet is constant. The other one compare E from simulation and E from calculation, and gets a accordant result.

CHAPTER 4: CHARACTERIZATION OF NANOFIBERS

4.1 Influence of Voltage on Thickness of Nanofibers

Experimentally, we used electrostatic initiation with three different glass-tip sizes and voltages, then recorded the diameter of the fibers. In Figure 4.1 we observe how the fiber's thickness decreases with increasing voltage at a 550um working distance. In order to know why this happens, we observe figure 3.4 showing that with increasing voltage, the localized electric field also increases. This stronger electric field leads to a stronger electrical force that stretches the nanofibers into thinner diameters.

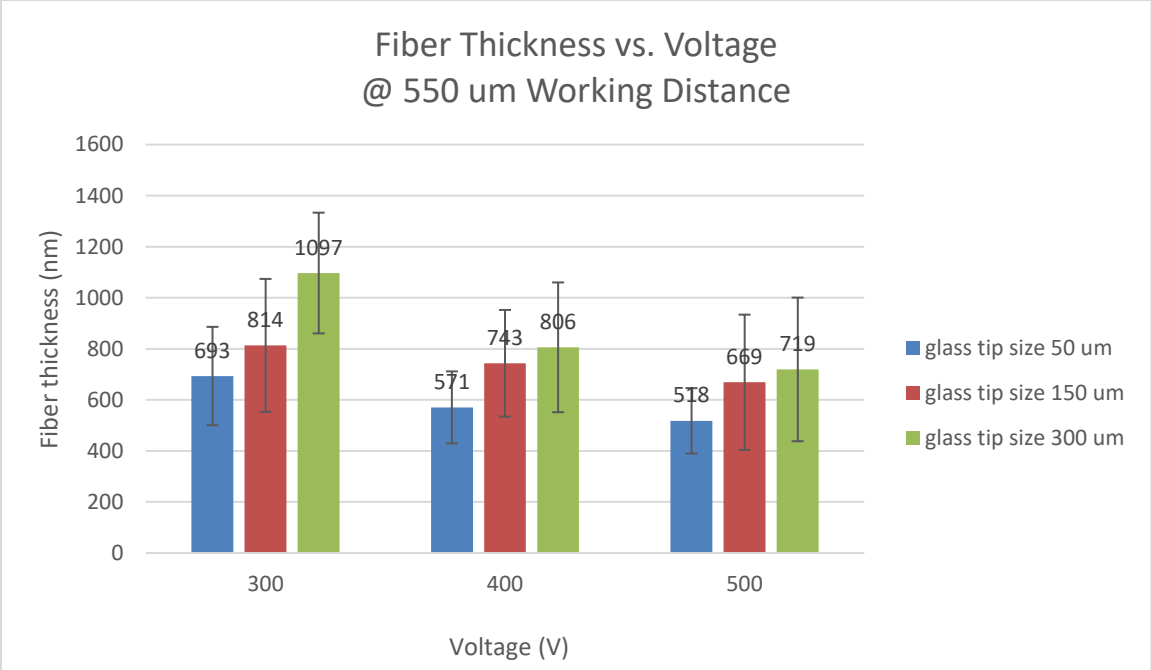

Figure 4.1. Measured fiber's diameter for three different glass tip sizes

4.2 Influence of glass size on Thickness of Nanofibers

In figure 4.1 the influence of the glass tip size can be observed, where a larger glass-tip size results in thicker fibers. Thus, towards thinner fibers voltages between 500 and 700 V, and

glass tip size below 50 μm are desired. What is the reason for thinner fibers with thinner glass tips? From our model, in figure 4.2 it is shown that, at a certain voltage, the critical electrical field are almost the same regardless of the glass tip size. Which means no matter how thick the glass tip is, when the electric field reached a critical value, the surface tension will be broken and nanofiber will be ejected. Thus, we conclude that the glass-tip size doesn't have a significant effect on the critical electric field value that initiates jet electrospinning.

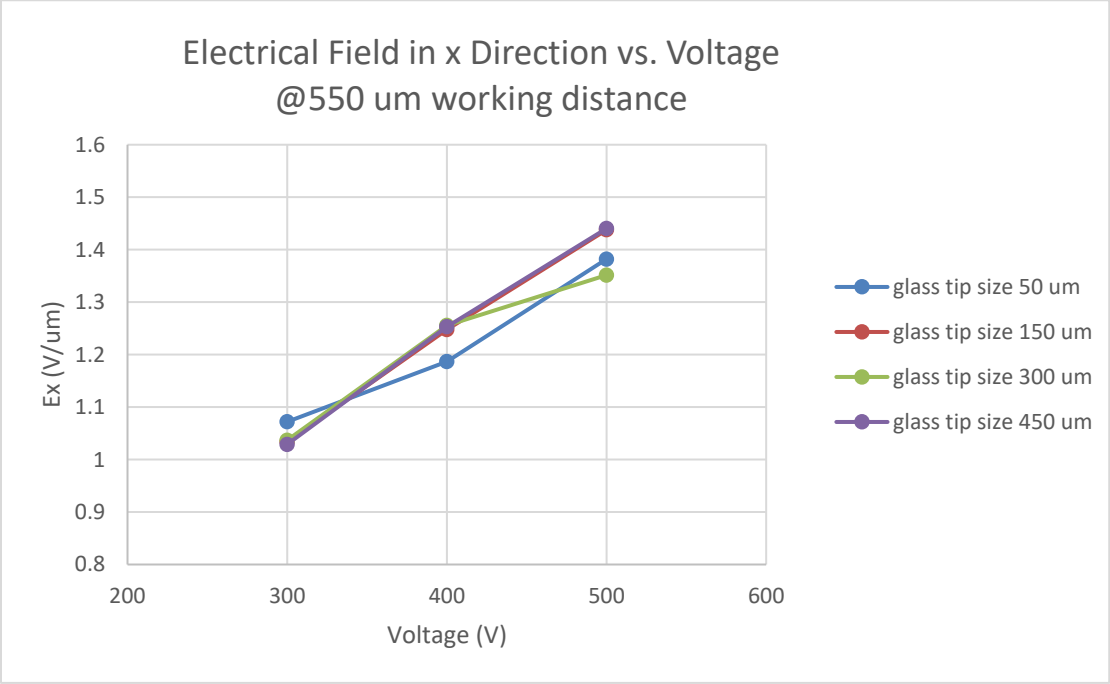

Figure 4.2. Simulated localized electric field at critical initiation point for different glass-tips.

Then we study the distribution of electrical field to search the reason why thickness of glass-tip influence characterization of nanofibers. In figure 4.3 the distribution of electric field with 50um and 450um glass tip respectively it's shown, for a droplet to substrate

distance of 550 µm and an applied voltage of 300v. For the 50 µm glass tip, the electric field it's more localized between the droplet and the glass tip. While for the 450 µm glass tip a larger area of the droplet will be influenced, resulting in thicker fibers.

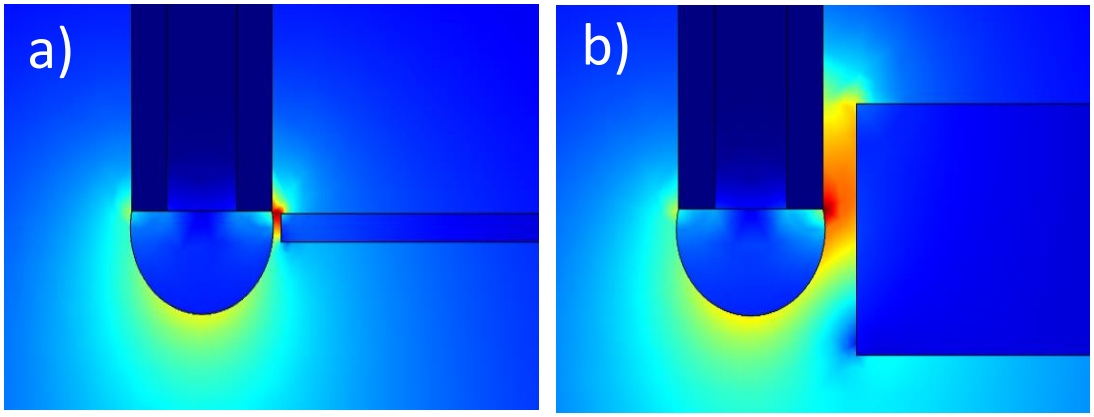

Figure 4.3. Simulated localized electric field for a) glass tip of 50µm; and b) glass tip of 450µm.

4.3 Influence of working distance on Thickness of Nanofibers

Experiments to observe the influence of the distance from the droplet to the grounded substrate were conducted and the diameter of the resulting fibers measured. The results are shown in figure 4.4, where it is seen that with a larger working distance, the thickness of the fiber it's thinner.

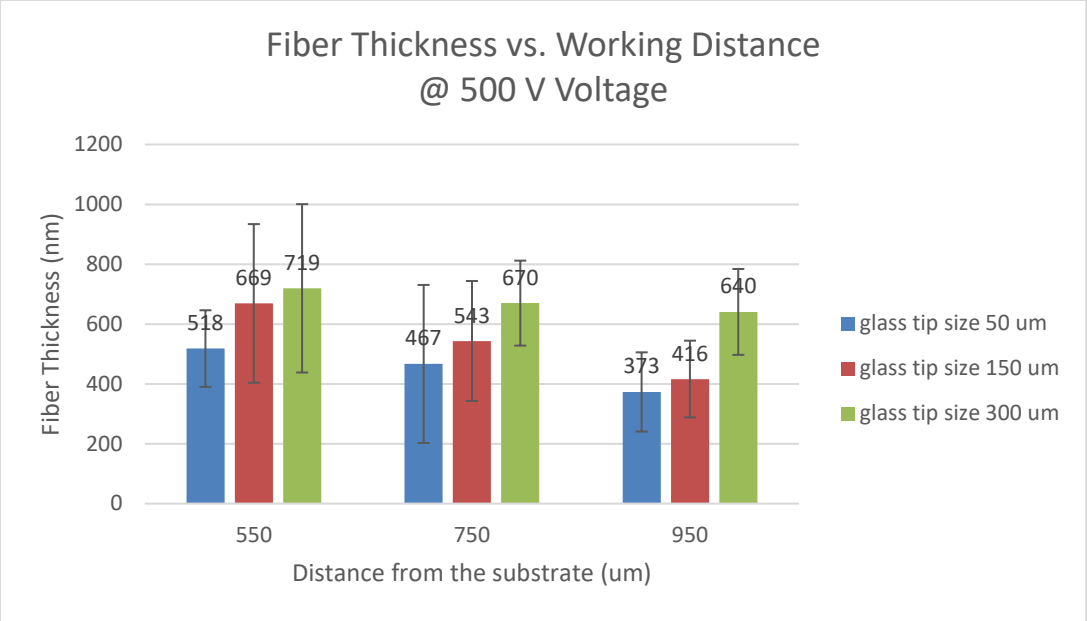

Figure 4.4. Measured fiber's diameter for three different glass tip sizes.

To explain the results of figure 4.4, the simulation of figure 4.6 now considers the electric field between the droplet and the substrate (y-axis). In this case, for a given voltage and glass tip size, the distribution of electrical field and electric field in the x-direction around the critical point are almost the same. However, changing the distance from the substrate will result in a reduction of the electrical field in the y-direction. Larger E_y will lead to larger fibers since this field gives the nanofiber a downward force (figure 4.5), which thickens the nanofiber.

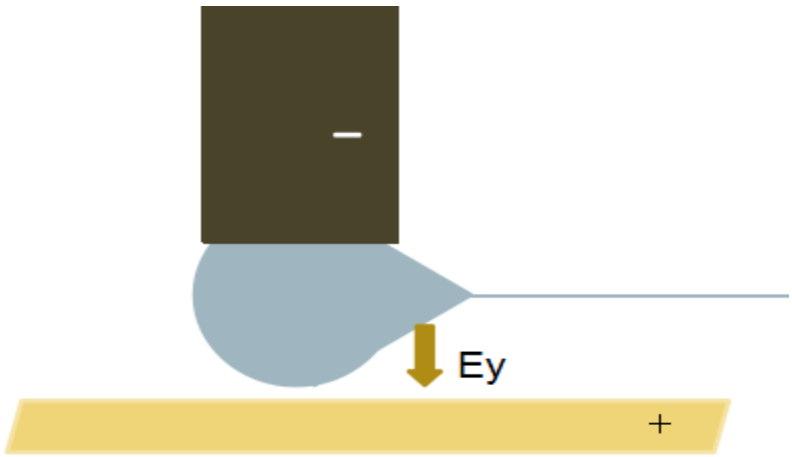

Figure 4.5. Force analysis at critical point

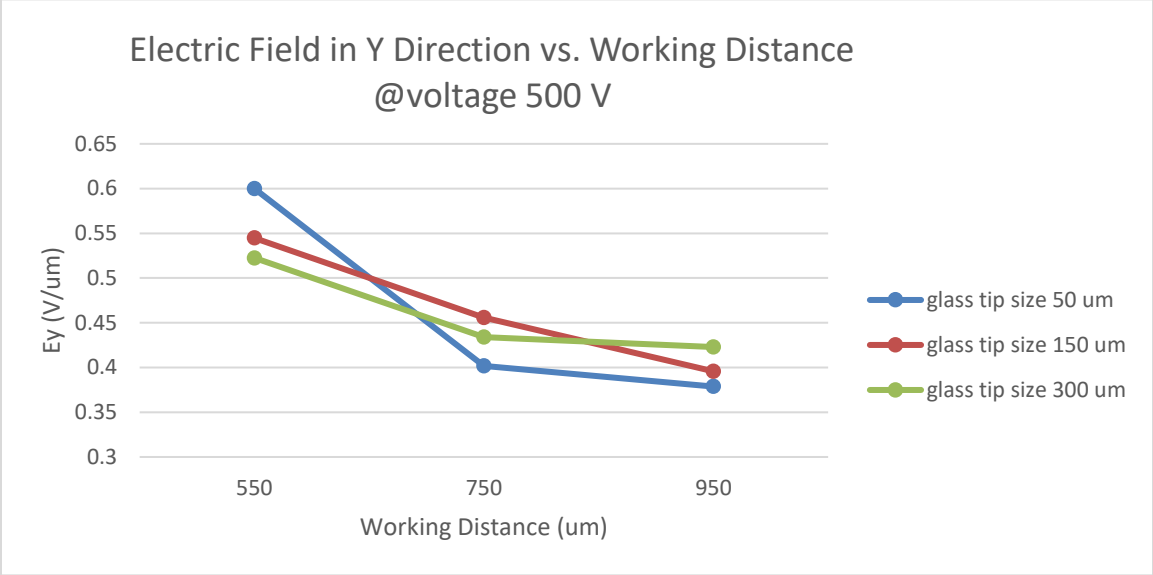

Figure 4.6. Electric field between droplet and substrate (y-axis) vs. working distance

4.4 Influence of Droplet Size on Thickness of Nanofibers

Experimentally it was found that the size of droplet will also affect the thickness of the droplet. As expected, a big droplet tends to generate a thicker fiber (figure 4.7). As the results shows in the simulation (figure 4.8), the electric field in the x-direction at the critical point for a small droplet it's larger than that for a bigger droplet. Therefore, a

smaller droplet will have a stronger electric force to stretch the nanofiber. This result shows the same conclusion as doing experiment with different voltage, where a larger Ex lead a thinner fiber.

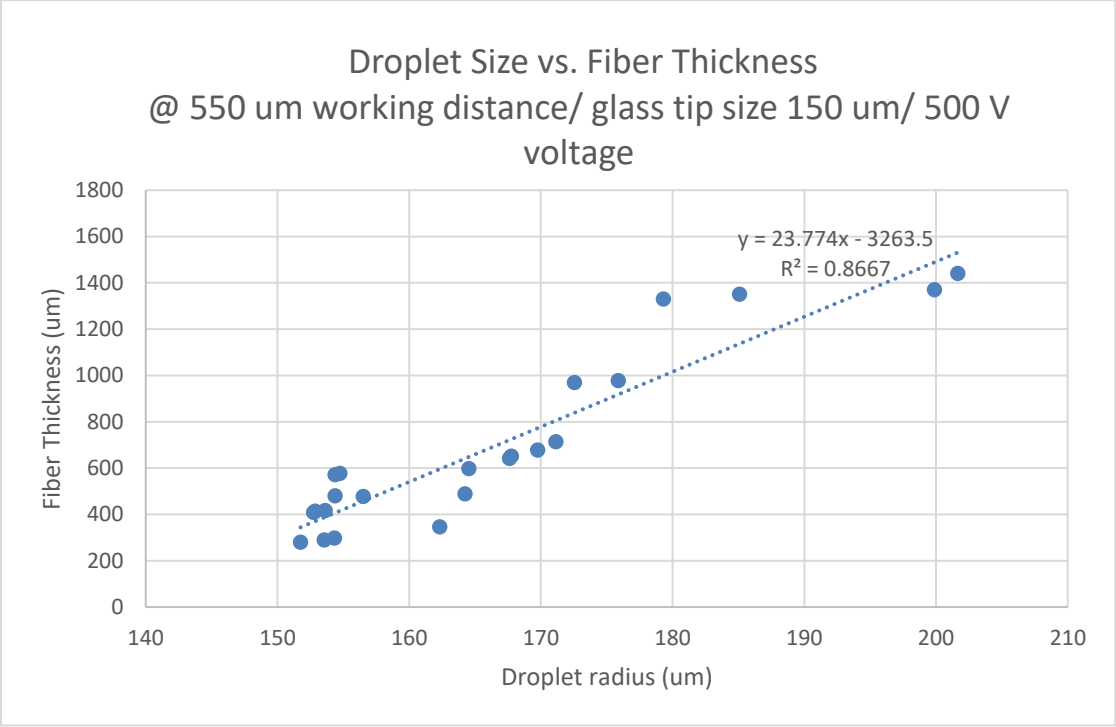

Figure 4.7. Measured fiber's diameter vs. droplet radius.

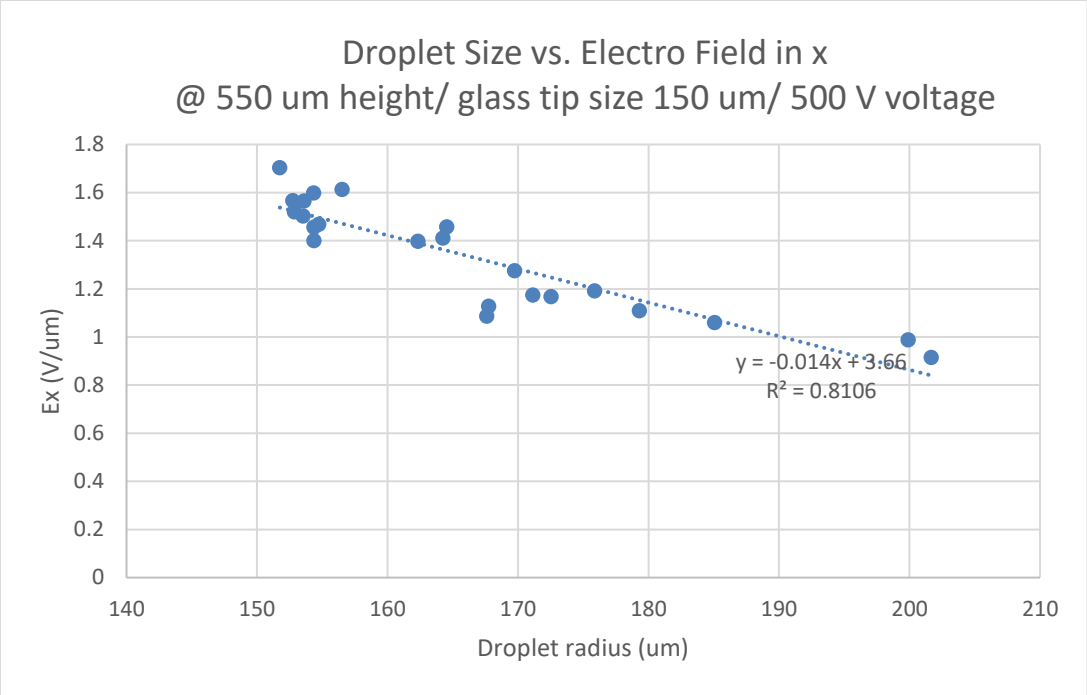

Figure 4.8. Simulated electric field in x-direction vs. droplet radius

4.5 Conclusion:

This chapter illustrates that thickness of nanofibers change under different conditions. In this chapter, we studies influence of glass-tip size, droplet size, voltage applied on needle and working distance on thickness of nanofibers. As experiments show:

1. The fiber's thickness decreases with increasing voltage, because a stronger electric field leads to a stronger electrical force that stretches the nanofibers into thinner diameters
2. A larger glass-tip size results in thicker fibers. the electric field of thinner glass-tip induced is more localized between the droplet and the glass tip. While for the thicker glass-tip a larger area of the droplet will be influenced, resulting in thicker fibers.
3. A big droplet tends to generate a thicker fiber. The reason why this happen is because the electric field in the x-direction at the critical point for a small droplet it's larger than

that for a bigger droplet, so a smaller droplet will have a stronger electric force to stretch the nanofiber, result in thinner nanofibers.

4. With a larger working distance, the thickness of the fiber it's thinner, because larger E_y will lead to larger fibers, this field gives the nanofiber a downward force, which thickens the nanofiber.

CHAPTER 5: PREDICTABILITY OF NFES SYSTEM

5.1 Predictability of NFES System

Based on the simulation and experimental results, we can now predict the critical distance required between the droplet and glass tip to initiate the jet.

Taking the fit value of the critical electric field in the x-direction (figure 3.6), we can get a good predictability of critical electrical field *Ex* since the R of fitting line is only 0.0024 and 0.0028. However, since electrical field in not visible, prediction of critical electrical field is hard to achieve control the initiation process directly. We hope to get a prediction of critical distance so we can know at what distance initiation will happen moving glass-tip towards polymer droplet under certain experimental conditions.

In order to achieve this goal, we extract fitting values on the line of simulation electrical field and calculation electrical field from figure 3.6, and insert those fitting lines into our FEA model to get a fitting critical distance and results are shown in figure 5.1. Those results matched the experimental well, which means our model has a good correspondence between critical distance and critical electrical field, and can be used in getting a good prediction of critical distance to realize control on initiation process.

In conclusion, when there is a need to predict when the initiation will happen under a certain condition. First do several experiments in condition easy to reach such as low voltage, then use our model to get a fitting line of critical electrical field. Extract the electrical field at certain condition and then insert in back to the model to get the predicted critical distance.

This design can get a better control of the NFES initiation process. Based on several groups of experiments, it can predict whole initiation process automatically, which benefit to the

automation and commercialization of NFES, and bring NFES technology from lab to human being's life.

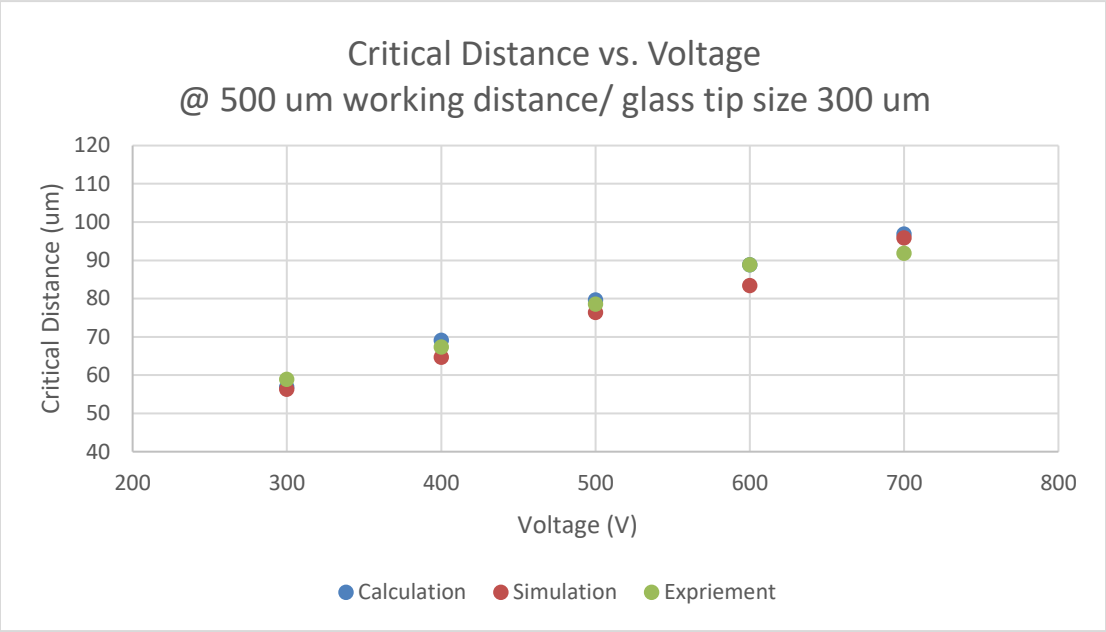

Figure 5.1. Table Critical Distance vs. Voltage

5.2 Conclusion:

This chapter shows that by inserting E from calculation and simulation into FEA model, the output critical distance match the experimental value very well. Our FEA model has a good predictability of NFES system and will benefit the automation and commercialization of whole process.

CHAPTER 6: CONCLUSION AND FUTURE WORK

6.1 Conclusion

Near-field electrospinning allows nanofibers to be written into specific pattern without bending instability. It is also much cheaper and safer than the traditional far-field electrospinning. This thesis first compares different kinds of initiation mode of near field electrospinning to see the influence on thickness of nanofiber and success rate. Secondly, we build a viable numerical simulation mold to simulate the electrical field around droplet. we induce two way to prove the feasibility of our FEA model. One of them proves surface tension of droplet is constant to show the model is right indirectly. The other one compare E from simulation and E from calculation, and gets an accordant result. Rest of studies are based on this simulation model. In addition, we study the characterization of nanofibers with key parameters changing, key parameters refer to initiation tip size, voltage, working distance and droplet size. The result shows a regular tendency between thickness of fibers and those key parameters:

1. The fiber's thickness decreases with increasing voltage.
2. A larger glass-tip size results in thicker fibers.
3. A big droplet tends to generate a thicker fiber.
4. With a larger working distance, the thickness of the fiber it's thinner.

This result will help us get better control of nanofibers and apply NFES to other fields easier. Finally, we use our FEA mode to see the predictability of whole process. And transfer the output from invisible electrical field into visible critical distance. Using this model, we will know how much critical distance and voltage a nanofiber needs to start jet

initiation process, which will be helpful for the automation and commercialization of NFES process.

However, our study still has some limitation. There is a threshold for reduction of thickness of nanofibers by changing key parameters such as increasing voltage. The essential solution for this problem is changing characterization of polymer solution directly. Therefore, in the future we will mainly focus on changing ratio of components in our solution or using other solutions to get a thinner nanofiber. In Addition, when two charge nanofibers get too close, the will repulse to each other result in a large gap between nanofibers. This slight bending will decrease the resolution of nanofiber pattern, which is also a problem waiting to be solved in the future.

REFERENCE

[1] Sun, Daoheng, et al. "Near-field electrospinning." Nano letters 6.4 (2006): 839-842.
[2] Reneker, Darrell H., et al. "Bending instability of electrically charged liquid jets of polymer solutions in electrospinning." Journal of Applied physics 87.9 (2000): 4531-4547.
[3] Yarin, Alexander L., S. Koombhongse, and Darrell Hyson Reneker. "Bending instability in electrospinning of nanofibers." Journal of Applied Physics 89.5 (2001): 3018-3026.
[4] Zheng, Gaofeng, et al. "Precision deposition of a nanofibre by near-field electrospinning." Journal of Physics D: Applied Physics 43.41 (2010): 415501.
[5] Chang, Chieh, Kevin Limkrailassiri, and Liwei Lin. "Continuous near-field electrospinning for large area deposition of orderly nanofiber patterns." Applied Physics Letters 93.12 (2008): 123111.
[6] Bisht, Gobind S., et al. "Controlled continuous patterning of polymeric nanofibers on three-dimensional substrates using low-voltage near-field electrospinning." Nano letters 11.4 (2011): 1831-1837.
[7] Canton, Giulia., et al. “Improved conductivity of suspended carbon fibers through integration of C-MEMS and Electro-Mechanical Spinning technologies.” Carbon 71 (2014). 338-342.
[8] Salazar, Arnoldo., et al. “Nanogap fabrication by Joule heating of electromechanically spun suspended carbon nanofibers.” Carbon 115 (2017). 811-818.
[9] Formhals, A. "Process and apparatus for preparing artificial threads: US, 1975504.(1934)."
[10] Huang, Zheng-Ming, et al. "A review on polymer nanofibers by electrospinning and their applications in nanocomposites." Composites science and technology 63.15 (2003): 2223-2253.
[11] Li, Dan, and Younan Xia. "Electrospinning of nanofibers: reinventing the wheel?." Advanced materials 16.14 (2004): 1151-1170.
[12] Reneker, Darrell H., and Iksoo Chun. "Nanometre diameter fibres of polymer, produced by electrospinning." Nanotechnology 7.3 (1996): 216.
[13] Theron, S. A., et al. "Multiple jets in electrospinning: experiment and modeling." Polymer 46.9 (2005): 2889-2899.
[14] Matthews, Jamil A., et al. "Electrospinning of collagen nanofibers." Biomacromolecules 3.2 (2002): 232-238.
[15] Kim, Jong‐Sang, and Darrell H. Reneker. "Polybenzimidazole nanofiber produced by electrospinning." Polymer Engineering & Science 39.5 (1999): 849-854.
[16] Li, Dan, Yuliang Wang, and Younan Xia. "Electrospinning of polymeric and ceramic nanofibers as uniaxially aligned arrays." Nano letters 3.8 (2003): 1167-1171.
[17] Huang, Zheng-Ming, et al. "A review on polymer nanofibers by electrospinning and their applications in nanocomposites." Composites science and technology 63.15 (2003): 2223-2253.
[18] Bisht, Gobind S., et al. "Controlled continuous patterning of polymeric nanofibers on three-dimensional substrates using low-voltage near-field electrospinning." Nano letters 11.4 (2011): 1831-1837.

[19] Kim, Hyojun., et al. “Onset condition of pulsating cone-jet mode of electrohydrodynamic jetting for plane, hole, and pin type electrodes.” Journal of Applied Physics 108 (2010). 102804.
[20] Saville, D. A. "Electrohydrodynamics: the Taylor-Melcher leaky dielectric model." Annual review of fluid mechanics 29.1 (1997): 27-64.
[21] Bentenitis, Nikolaos., et al. “Droplet Deformation in Dc Electric Fields: The Extended Leaky Dielectric Model”. Langmuir 21 (2005). 6194–6209.
[22] Bamji, S. S., A. T. Bulinski, and K. M. Prasad. "Electric field calculations with the boundary element method." IEEE Transactions on Electrical Insulation 28.3 (1993): 420-424.